Spectroellipsometric study of sol–gel derived potassium sodium strontium barium niobate films

C. L. Mak, B. Lai, K. H. Wong, C. L. Choy, D. Mo et al.

Related Articles

Additional information on J. Appl. Phys.

Spectroellipsometric study of sol–gel derived potassium sodium strontium barium niobate films

C. L. Mak,[a] B. Lai, K. H. Wong, C. L. Choy, D. Mo,[b] and Y. L. Zhang[b]
Department of Applied Physics and Materials Research Center, The Hong Kong Polytechnic University, Hung Hom, Hong Kong Special Administrative Region, People's Republic of China

Spectroscopic ellipsometry (SE) was used to characterize the sol–gel derived $(K_{0.5}Na_{0.5})_{0.4}(Sr_{0.6}Ba_{0.4})_{0.8}Nb_2O_6$ (KNSBN) thin films as a function of sol concentration. In the analysis of the measured SE spectra, a modified double-layer Forouhi–Bloomer model was adopted to represent the optical properties of the KNSBN films. In this model, the films were assumed to consist of two layers—a bottom bulk KNSBN layer and a surface layer that composed of bulk KNSBN as well as void. Good agreement was obtained between the measured spectra and the model calculations in the chosen spectral region. Effective medium approximation theory was used to evaluate the effective refractive index for the surface layer. The results of SE have been correlated with atomic force microscopy measurements of surface roughness. Our analyses have shown that the surface layer had a lower refractive index than the bottom one. In addition, the refractive index and the surface roughness of the KNSBN films increase with the sol concentration. © *2001 American Institute of Physics.* [DOI: 10.1063/1.1355283]

I. INTRODUCTION

In recent years, ferroelectric materials have been explored to manufacture various optical thin film devices. Among different ferroelectric materials, potassium sodium strontium barium niobate (KNSBN) has been reported to have high electro-optic coefficient (59×10^{-12} m/V),[1] large transparent range (from 400 nm to 5.6 μm),[1] high threshold energy for optical damage (618 MW/cm^2),[1] and Curie temperature of above 200 °C.[2] These properties make KNSBN an ideal material for many optical device applications such as an electro-optic switch[3] and an optical waveguide.[4] However, despite these outstanding properties, few studies on the KNSBN films have been reported.[5]

Thin film fabrication techniques based on the sol–gel method has the advantages of excellent homogeneity, ease of chemical composition control, high purity, low processing temperature, and uniformity over large area. Furthermore, the sol–gel process is capable of producing high-quality films of a few microns thick that are difficult to prepare using physical deposition methods. As films of a few microns thick are required in many optical device applications, it will be beneficial to study the formation processes of sol–gel derived films and their corresponding optical properties. Sol–gel thick films are generally obtained using either high concentration sol or multilayer coating. The former scheme is obviously more economical in time and effort. Unfortunately, cracks are generally resulted if the sol concentrations exceed certain limit. In this article, the effects of sol concentration on refractive index (n), extinction coefficient (k), and surface roughness are investigated. We demonstrate that sol–

gel derived KNSBN films of good structural and optical qualities can be fabricated with sols of concentration less than 0.2 M.

Spectroscopic ellipsometry (SE) is a nondestructive technique using light reflection. In conjunction with computer modeling of the experimental data, SE is capable of depth profiling of thin film samples with depth resolution in the angstrom range. Therefore, SE becomes a powerful technique for optical thin films characterization and has been extensively used by physicists, chemists, electrochemists, electrical and chemical engineers.[6] The complex Fresnel reflection coefficient, which is composed of factors related to amplitude and phase difference of polarized light before and after reflection, can be expressed as[7]

$$\frac{R_p}{R_s} = \tan \Psi e^{i\Delta} \tag{1}$$

where R_p and R_s are the reflection coefficients for light polarized parallel (p) and perpendicular (s) to the plane of incidence respectively, and are complex functions of refractive index n and extinction coefficient k. Generally, SE measures the traditional ellipsometric angles, ψ and Δ, as functions of energy in the experiment. However, in this study, spectroscopic phase modulated method was used.[8] The incident light beam was polarized before reflecting from the sample. The reflected beam, after passing through a photoelastic modulator (M) and an analyzer (A), was dispersed by a monochromator and detected by a photomultiplier tube. The orientations (with respect to the plane of incidence) of the polarizer, modulator, and analyzer are denoted P, M, and A, respectively. The photoelastic modulator consisted of a fused silica block sandwiched between piezoelectric quartz crystals oscillating at a frequency of ~50 kHz. This generated a pe-

---

[a]Electronic mail: apaclmak@polyu.edu.hk
[b]Also at: Department of Physics, Zhongshan University, Guangzhou 510275, People's Republic of China.

riodic phase shift $\delta(t)$ between orthogonal amplitude components of the transmitted beam. The detected intensity, in this case, would take the general form:[8]

$$I(t) = I[I_0 + I_S \sin \delta(t) + I_C \cos \delta(t)], \tag{2}$$

where I is a constant, and

$$\begin{aligned} I_0 = 1 &- \cos 2\psi \cos 2A + \cos 2(P-M)\cos 2M \\ &\times (\cos 2A - \cos 2\psi) + \sin 2A \cos \Delta \cos 2(P-M) \\ &\times \sin 2\psi \sin 2M, \end{aligned} \tag{3}$$

$$I_S = \sin 2(P-M)\sin 2A \sin 2\psi \sin \Delta, \tag{4}$$

$$\begin{aligned} I_C = \sin 2(P-M)[&\sin 2M(\cos 2\psi - \cos 2A) \\ &+ \sin 2A \cos 2M \sin 2\psi \sin \Delta]. \end{aligned} \tag{5}$$

For a suitable choice of angle A, M, and P, a simple determination of the ellipsometric angles from I_0, I_S and I_C could be obtained. Throughout the experiment, we set

$$P-M = +45°; \quad M = 0° \quad \text{and} \quad A = +45° \tag{6}$$

so that

$$\begin{aligned} I_0 &= 1, \\ I_S &= \sin 2\psi \sin \Delta, \\ I_C &= \sin 2\psi \cos \Delta. \end{aligned} \tag{7}$$

Therefore, we could calculate ψ and Δ accurately by obtaining I_S and I_C.

II. EXPERIMENTAL PROCEDURE

The precursors for the KNSBN sol were strontium metal, barium metal, sodium ethoxide, potassium hydroxide, and niobium chloride. Firstly they were dissolved separately in 2-methoxyethanol, which acted as both the solvent and sol stabilizer, to form the corresponding metal alkoxides. The different metal alkoxides were mixed together to form the KNSBN sol according to the desired stoichiometric ratio of K:Na:Sr:Ba:Nb = 0.2:0.2:0.48:0.32:2. The final KNSBN sol, which was yellowish brown in color and free of suspension,

$$k(E) = \frac{A(E_g - E)^2}{E^2 - BE + C}, \quad n(E) = n_\infty + \frac{A(-B^2 E + 2E_g BE - 2E_g^2 E + 2CE + E_g^2 B + BC - 4E_g C)}{\sqrt{4C - B^2}(E^2 - BE + C)}, \tag{8}$$

where E_g is the gap energy, n_∞ is the refractive index at infinity energy, and *A, B,* and *C* are positive constants. Here, E represents the energy ranging from 2.0 to 4.5 eV (620 nm to 276 nm). The SE derived film thickness was compared with the data measured by a surface profiler (KLA-Tencor P-10). The films surface roughness was, on the other hand, measured by an atomic force microscope [(AFM), METRIS-2000] and the results were correlated to the SE analysis.
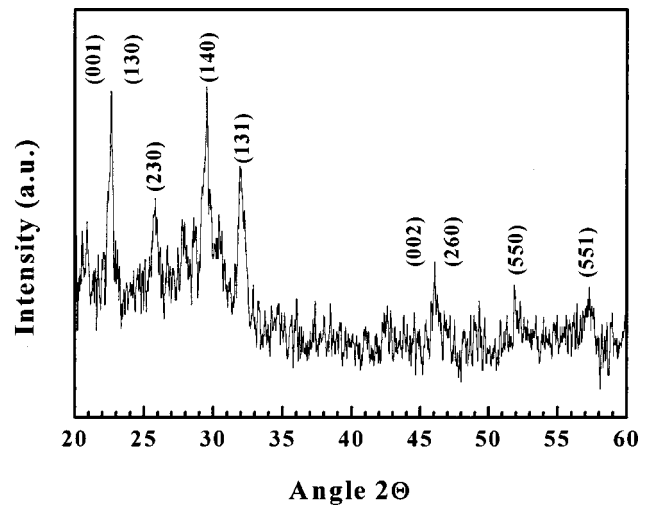

FIG. 1. XRD spectrum of single layer KNSBN film of 0.18 M sol concentration. The film was annealed at 700 °C for 2 h.

was refluxed at 120 °C to desired sol concentrations of 0.03, 0.06, 0.09, 0.12, 0.15, 0.18, 0.21, and 0.24 M. These sols of different concentrations were dip coated onto $1 \times 2\ \text{cm}^2$ single crystal (100)Si wafers. The withdrawn rate was fixed at 0.3 cm/s using a motorized translator. The films were then air dried for about 20 min and then annealed at 700 °C for 2 h. Details of the procedure can be found elsewhere.[9]

The crystalline structures of the sol–gel KNSBN films were analyzed by an x-ray diffractometer [(XRD) Philip X'pert] with Cu $K\alpha$ radiation. Ellipsometric measurements were carried out by a spectroscopic phase modulated ellipsometer (Jobin Yvon UVISEL) in the energy range of 2.0–4.5 eV at 10 meV intervals. All measurements were performed at a 70° angle of incidence with the analyzer and modulator set at 45° and 0°, respectively. The obtained spectra were best fitted using the Forouhi–Bloomer model.[10] The parameters, including the thickness of the films, obtained from each of the fittings were used to simulated n and k by the following dispersion relations:[10]

III. RESULTS AND DISCUSSIONS

Figure 1 shows a typical XRD spectrum of the $(K_{0.5}Na_{0.5})_{0.4}(Sr_{0.6}Ba_{0.4})_{0.8}Nb_2O_6$ (KNSBN) films with sol-concentration of 0.18 M. From the figure, peaks corresponding to the tetragonal tungsten bronze (TTB) phase KNSBN were identified.[9] No orthorhombic $SrNb_2O_6$ ($2\theta = 29.1°$) or $BaNb_2O_6$ ($2\theta = 28.5°$) phases[11] were observed. This implies that a completely crystallized TTB structure was obtained
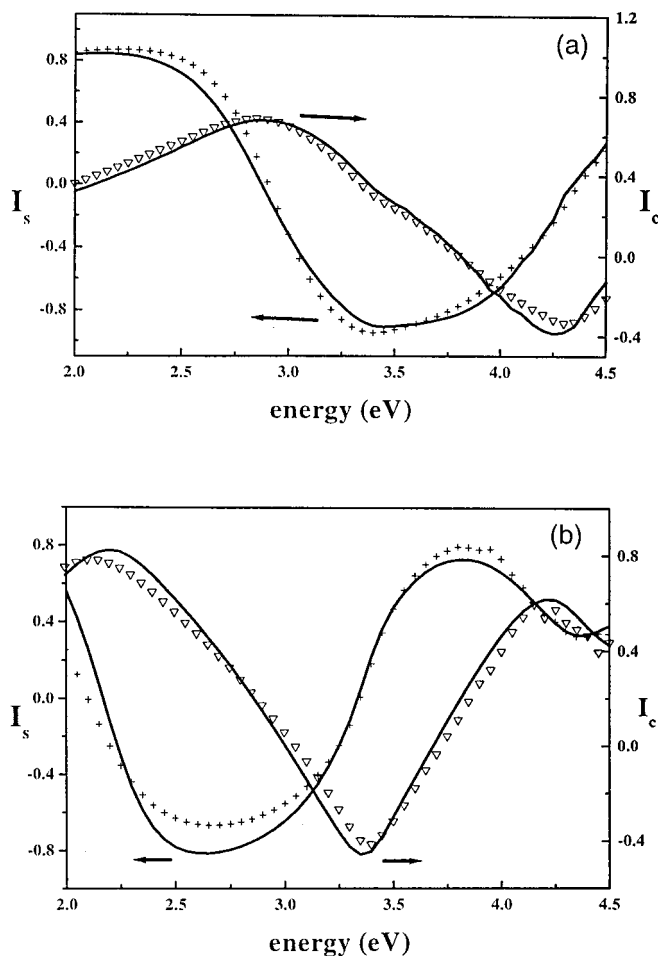
FIG. 2. Spectra of the ellipsometric parameters I_S and I_C as a function of photon energy, obtained from SE experiments for KNSBN films of (a) 0.09 M and (b) 0.15 M sol concentration. The $+$ and ∇ are the measured I_S and I_C values respectively, while the solid lines are obtained from fitting.

with annealing temperature as low as 700 °C. Similar results were also observed in films with lower sol concentrations, although weaker diffraction peaks were obtained due to smaller film thickness. Therefore, we conclude that TTB phase KNSBN were obtained in all of the films with different sol concentration.

Dispersion curves of I_S and I_C for KNSBN films with sol concentrations equal to 0.09 and 0.15 M are shown in Figs. 2(a) and 2(b), respectively. The spectra show oscillations due to film thickness. For films fabricated with sol of concentration larger than 0.18 M, microcracks were observed. This sets the upper limit on the sol concentration in which crack-free KNSBN sol–gel films can be obtained. General speaking, higher sol concentration results in thicker films. This is revealed by the more closely spaced oscillation observed in both the I_S and I_C spectra [Fig. 2(b)]. Our initial analysis was based on a single-layer Forouhi–Bloomer model. Poor agreement, however, was obtained with the experimental data. In subsequent analysis, we modified the single-layer Forouhi–Bloomer model into a double-layer Forouhi–Bloomer (DLFB) model. In this model, we assume that the films consist of two layers—a bottom bulk KNSBN layer and a surface layer that composed of bulk KNSBN as
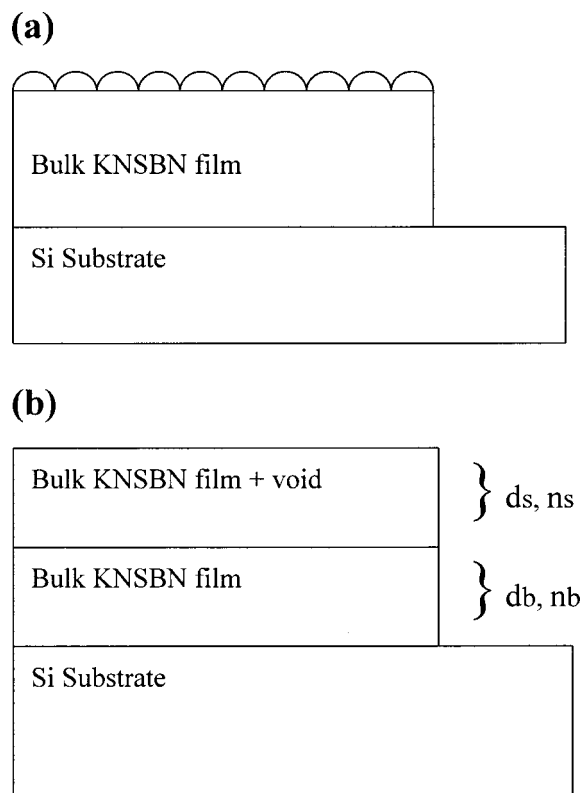

FIG. 3. Schematic picture of the DLFB model.

well as voids. These voids in the surface layer were mainly caused by surface roughness and porosity resulting from evaporation of the solvent in the annealing process.[12] Similar inhomogeneity has also been observed in $SrBi_2(Ta_{1-X}Nb_X)_2O_9$ (Ref. 13) and amorphous silicon–carbon alloy films.[14] Figure 3 shows the DLFB model for a single-layer KNSBN sol–gel film grown on a Si substrate. Based on this modified DLFB model, better-fit results were obtained. The solid lines in Figs. 2(a) and 2(b) denote these results. The volume fraction of void f, effective thickness of surface layer d_s and bottom layer d_b, and the other five parameters (A, B, C, E_g and n_∞) obtained by DLFB model are shown in Table I.

After securing the fitted parameters, the n and k dispersion spectra for the bottom KNSBN layers, evaluated using Eq. (8), are plotted in Figs. 4(a) and 4(b) as a function of sol concentration, respectively. The Bruggeman effective me-

TABLE I. The fitting parameters of the KNSBN films with different sol concentration.

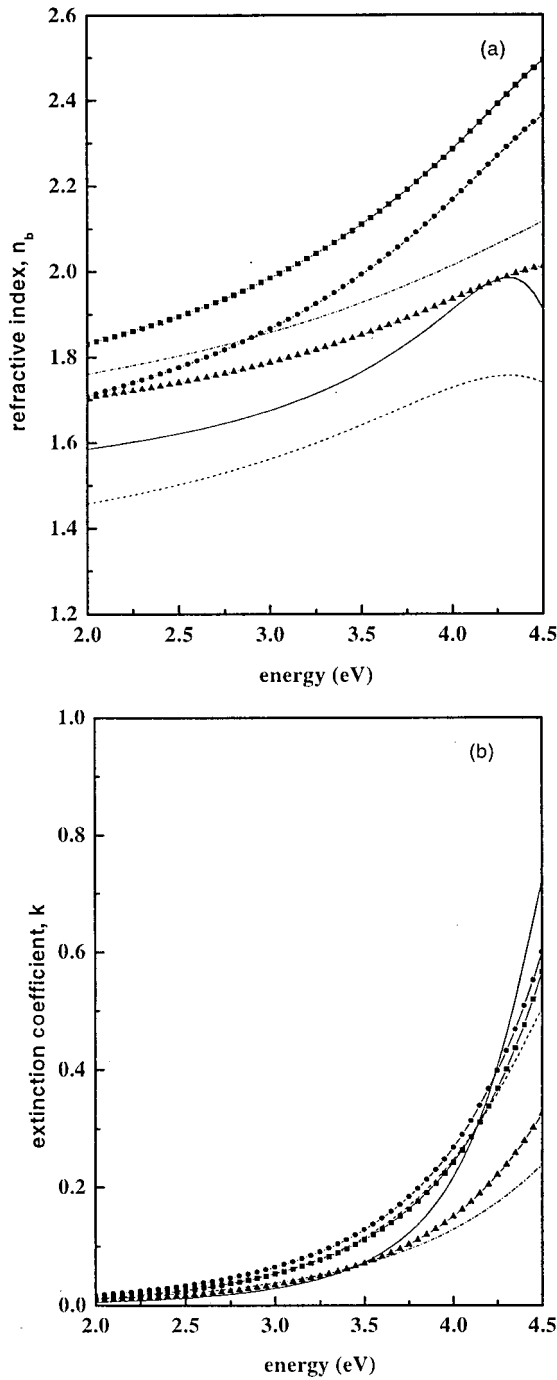| Sol concentration	0.03 M	0.06M	0.09 M	0.12 M	0.15 M	0.18 M
N_∞	1.396	1.170	1.469	1.316	1.264	1.402
A	0.033	0.105	0.075	0.199	0.105	0.104
B (eV)	9.28	9.40	10.08	11.09	10.38	10.37
C (eV^2)	21.87	23.69	27.01	34.88	28.17	28.04
E_g (eV)	1.82	1.79	1.84	1.86	1.78	1.78
d_b (nm)	29	60	69	87	89	105
d_s (nm)	3	6	8	10	20	80
Void percentage f (%)	10	40	45	50	50	50

FIG. 4. (a) The refractive index and (b) the extinction coefficient of the bottom KNSBN layers of 0.03 M (solid line), 0.06 M (dashed line), 0.09 M (dash-dot line), 0.12 M (solid line $+\blacktriangle$), 0.15 M (solid line $+\bullet$), 0.18 M (solid line $+\blacksquare$) sol concentration obtained by Eq. (8).
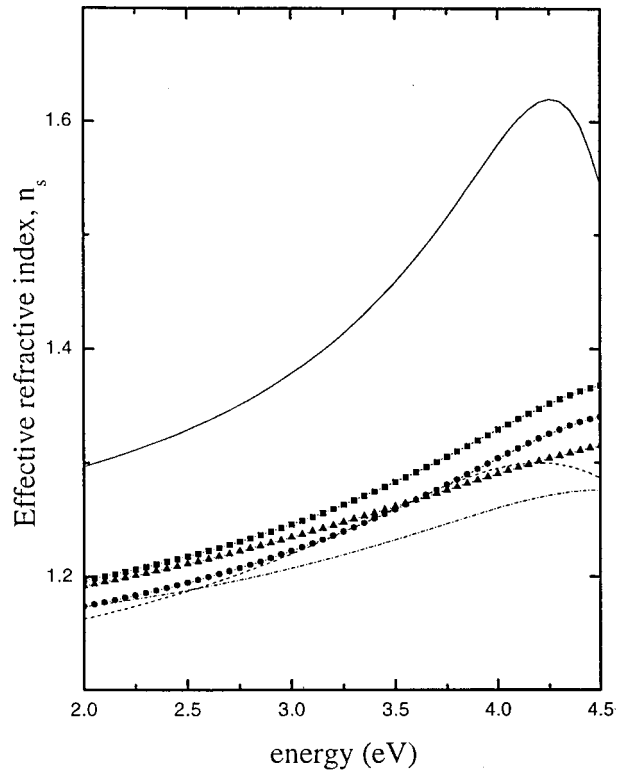

FIG. 5. Effective refractive index of the upper KNSBN layers of 0.03 M (solid line), 0.06 M (dashed line), 0.09 M (dash-dot line), 0.12 M (solid line $+\blacktriangle$), 0.15 M (solid line $+\bullet$), 0.18 M (solid line $+\blacksquare$) sol concentration obtained by EMA.

dium approximation (EMA)[15] was used to describe the n dispersion spectra for the top KNSBN layers, which is expressed by

$$(1-f)\frac{n_b^2-n_s^2}{n_b^2+2n_s^2}+f\frac{1-n_s^2}{1+2n_s^2}=0, \qquad (9)$$

where n_b is the refractive index of the bottom layer (i.e., the bulk KNSBN) and n_s is the effective refractive index of the

surface layers. Figure 5 shows the n_s dispersion spectra as a function of sol concentration for the upper KNSBN layers.

In general, the refractive indices n_s and n_b of the KNSBN films increase with energy. For example, the refractive index of the bottom layer n_b of the 0.06 M sample rises from 1.46 (at 2.0 eV) to 1.75 (at 4.4 eV) as observed in Fig. 4(a). As the sol concentration increases, the spectra shift upward indicating that the refractive index increases with sol concentration. For instance, when the sol concentration is 0.18 M, the refractive index n_b of the bottom KNSBN layer is about 1.97 at 2.9 eV. The escalation of n_b with concentration may simply be a result of increasing density. Further investigation of the effect of sol concentration on the density of the film using transmission electron microscope will be of importance. Similarly, n_s also increases with the sol concentration except the 0.03 M films. According to the EMA, a larger void fraction leads to a lower effective refractive index for the upper layer. This explains why the surface layers of 0.03 M films have a larger refractive index than the surface layers of other films.

Based on the fitting parameter in Table I, we see that both the ratio of surface layer/bottom layer (d_s/d_b) and the void percentage increase with sol concentration. These results demonstrate that the sol–gel film surface gets rougher at higher sol concentration. This phenomenon is confirmed by AFM measurements of the surface roughness (R_q) of the film as a function of sol concentration (Fig. 6). All AFM images of 5×5 μm^2 scan area were collected in the tapping mode with etched c-Si tips. The inset shows the relationship
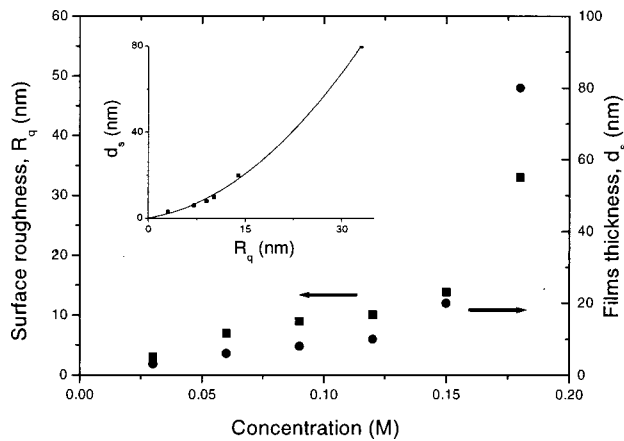
FIG. 6. Root mean square surface roughness (R_q) and film thickness (d_S) with different sol concentration obtained by AFM and fitting of the SE spectra. The scan area of the AFM measurement is 5 μm×5 μm. Inset shows the relationship between R_q and d_S.

FIG. 7. Films thickness obtained by fitting from ellipsometer (●, $d_S + d_b$) and surface profiler (■) as a function of sol concentration.

between d_s and R_q. J. Koh *et al.* correlated the results of SE and AFM measurements of surface roughness on amorphous semiconductor thin films.[14] In their studies, a similar approach, based on a two-layer optical model consisting of surface and bulk layers was used to evaluate the surface roughness. The refractive index of the surface layer was modeled using Eq. (9) with fixed void percentage of 50%. A relationship of the form: $d_s(\text{SE}) = 1.5R_q + 0.4$ nm was obtained. However, they confined their studies to high quality dense films with very small surface roughness (~0.3% of the total thickness). The voids were assumed to originate from surface roughness only. In our sol–gel derived films, however, voids are contributed from both the surface roughness and pores in the bulk due to the evaporation of solvent.[12] Therefore, we let the void percentage be a fitting parameter to account for void from both surface roughness as well as solvent evaporation. From Table I, we observed that the void percentage increases with the sol concentration and saturated at 50% for sol of 0.12 M. This indicates that at low concentration the surface roughness is small so that the contribution is mainly due to pores while at high concentration the void percentage is mostly due to the surface roughness. Unlike the relation obtained in semiconductor,[14] an modified correlation of ellipsometry and AFM measurements of surface roughness was observed in our measurement:

$$d_s(\text{SE}) \approx 0.059R_q^2 + 0.48R_q + 0.11 \text{ nm}. \qquad (10)$$

For small R_q i.e., smooth films, the first term on the right-hand side will be negligible so that Eq. (10) becomes a linear relation consistent with that obtained in Ref. 14. The difference in the slope may be simply due to different surface geometry existing in the surface of the film. Detailed investigation of the correlation between the surface geometry and the value of the slope will be of great interest. As the films become rough, i.e., large R_q, the empirical relation given by Eq. (10) applies. Indeed the d_s/d_b ratios of our samples are much larger than those reported in Ref. 14 indicating that our sol–gel films are rougher. This is simply due to the different preparation method used. Finally, a sudden increase of sur-
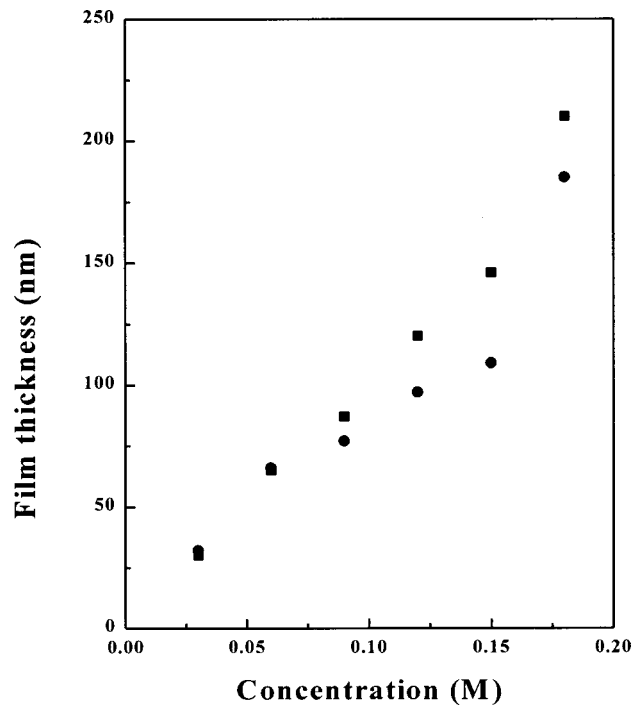
face roughness at 0.18 M may simply due to the fact that 0.18 M is very closed to the critical point of microcracks formation (occurs at about 0.2 M).

Figure 7 plots the relation between the fitted thickness of the film and sol concentration. The fitted results were compared with those measured by the surface profiler. Obviously, the thickness of the film, as expected, increases with sol concentration. The two sets of data are comparable to each other. However, the discrepancy seems to propagate as the film thickness is increased and can be attributed to the effect of increasing surface roughness with film thickness.

IV. CONCLUSION

The optical dispersion functions of the KNSBN films derived from different sol concentration were obtained by spectroscopic ellipsometry. In order to yield a more accurate optical constant of the KNSBN films, we use a modified Forouhi–Bloomer model, in which an effective surface layer representing the surface roughness and the pores in the bulk was visualized. The refractive indices of these surface layers were found, as expect, lower than the indices of the bottom layers. The SE fitted film thickness agrees well with those measured by the surface profiler. The thickness of the surface layer, on the other hand, is correlated to the AFM measurements of the root mean square of the surface roughness. Our results do suggest that the refractive indices of the sol–gel derived KNSBN films increase with the sol concentration.

ACKNOWLEDGMENTS

[1] Y. Xu, *Ferroelectric Materials and Their Applications* (Elsevier, New York, 1991).

[2] H. R. Xia, C. J. Wang, H. Yu, H. C. Chen and M. Wang, Jpn. J. Appl. Phys., Part 1 **36**, 2179 (1997).

[3] V. M. Fridkin, *Photoelectrics* (Springer, Berlin, 1979).

[4] D. K. Fork, F. Armani–Leplingard, and J. J. Kingston, Mater. Res. Bull. **31**, 53 (1996).

[5] G. Park, J. Sel, S. Bu, and I. H. Song, Solid State Commun. **111**, 125 (1999).

[6] K. Vedam, Thin Solid Films **313**, 1 (1998).

[7] D. Mo, *Solid State Optics* (Chinese Advanced Education Press, Beijing, 1996).

[8] S. N. Jasperson and S. E. Schnatterly, Rev. Sci. Instrum. **40**, 761 (1969).

[9] C. L. Mak, B. Lai, and K. H. Wong, J. Sol-Gel Sci. Technol. **18**, 129 (2000).

[10] A. R. Forouhi and I. Bloomer, Phys. Rev. B **34**, 7018 (1986).

[11] M. M. T. Ho, C. L. Mak, and K. H. Wong, J. Eur. Ceram. Soc. **19**, 1115 (1999).

[12] C. H. Luk, C. L. Mak, and K. H. Wong, Thin Solid Films **298**, 57 (1997).

[13] T. C. Chen, T. Li, X. Zhang, and S. B. Desu, J. Mater. Res. **12**, 2165 (1997).

[14] J. Koh, Y. Lu, C. R. Wronski, Y. Kuang, R. W. Collins, T. T. Tsong and Y. E. Strausser, Appl. Phys. Lett. **69**, 1297 (1996).

[15] D. A. G. Bruggeman, Ann. Phys. (Leipzig) **24**, 636 (1935).